

## Orbital and spin moments of 5 to 11nm Fe<sub>3</sub>O<sub>4</sub> nanoparticles measured via x-ray magnetic circular dichroism

Y. P. Cai, K. Chesnel, M. Trevino, A. Westover, R. G. Harrison, J. M. Hancock, S. Turley, A. Scherz, A. Reid, B. Wu, C. Graves, T. Wang, T. Liu, and H. Dürr

Citation: *Journal of Applied Physics* **115**, 17B537 (2014); doi: 10.1063/1.4869277

View online: <http://dx.doi.org/10.1063/1.4869277>

View Table of Contents: <http://scitation.aip.org/content/aip/journal/jap/115/17?ver=pdfcov>

Published by the [AIP Publishing](#)

---

### Articles you may be interested in

[Tuning exchange bias in Fe/-Fe<sub>2</sub>O<sub>3</sub> core-shell nanoparticles: Impacts of interface and surface spins](#)  
*Appl. Phys. Lett.* **104**, 072407 (2014); 10.1063/1.4865904

[Facile synthesis of single-phase spherical -Fe<sub>16</sub>N<sub>2</sub>/Al<sub>2</sub>O<sub>3</sub> core-shell nanoparticles via a gas-phase method](#)  
*J. Appl. Phys.* **113**, 164301 (2013); 10.1063/1.4798959

[Surface spin effects in La-doped CoFe<sub>2</sub>O<sub>4</sub> nanoparticles prepared by microemulsion route](#)  
*J. Appl. Phys.* **110**, 073902 (2011); 10.1063/1.3642992

[Orbital moment determination in \(Mn<sub>x</sub>Fe<sub>1-x</sub>\)<sub>3</sub>O<sub>4</sub> nanoparticles](#)  
*J. Appl. Phys.* **109**, 07B532 (2011); 10.1063/1.3562905

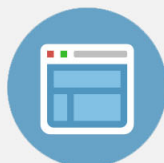
[Enhanced magnetism of Fe<sub>3</sub>O<sub>4</sub> nanoparticles with Ga doping](#)  
*J. Appl. Phys.* **109**, 07B529 (2011); 10.1063/1.3562196

---



## Re-register for Table of Content Alerts

Create a profile.



Sign up today!



## Orbital and spin moments of 5 to 11 nm Fe<sub>3</sub>O<sub>4</sub> nanoparticles measured via x-ray magnetic circular dichroism

Y. P. Cai,<sup>1</sup> K. Chesnel,<sup>1,a)</sup> M. Trevino,<sup>1</sup> A. Westover,<sup>1</sup> R. G. Harrison,<sup>2</sup> J. M. Hancock,<sup>2</sup> S. Turley,<sup>1</sup> A. Scherz,<sup>3</sup> A. Reid,<sup>3</sup> B. Wu,<sup>3</sup> C. Graves,<sup>3</sup> T. Wang,<sup>3</sup> T. Liu,<sup>3</sup> and H. Dürr<sup>3</sup>

<sup>1</sup>Department of Physics and Astronomy, Brigham Young University, Provo, Utah 84602, USA

<sup>2</sup>Department of Chemistry and Biochemistry, Brigham Young University, Provo, Utah 84602, USA

<sup>3</sup>SLAC National Accelerator Laboratory, Stanford Institute for Materials and Energy Science (SIMES), Menlo Park, California 94025, USA

(Presented 6 November 2013; received 23 September 2013; accepted 17 January 2014; published online 28 April 2014)

The orbital and spin contributions to the magnetic moment of Fe in Fe<sub>3</sub>O<sub>4</sub> nanoparticles were measured using X-ray magnetic circular dichroism (XMCD). Nanoparticles of different sizes, ranging from 5 to 11 nm, were fabricated via organic methods and their magnetic behavior was characterized by vibrating sample magnetometry (VSM). An XMCD signal was measured for three different samples at 300 K and 80 K. The extracted values for the orbital and spin contributions to the magnetic moment showed a quenching of the orbital moment and a large spin moment. The calculated spin moments appear somewhat reduced compared to the value expected for bulk Fe<sub>3</sub>O<sub>4</sub>. The spin moments measured at 80 K are larger than at 300 K for all the samples, revealing significant thermal fluctuations effects in the nanoparticle assemblies. The measured spin moment is reduced for the smallest nanoparticles, suggesting that the magnetic properties of Fe<sub>3</sub>O<sub>4</sub> nanoparticles could be altered when their size reaches a few nanometers. © 2014 AIP Publishing LLC. [<http://dx.doi.org/10.1063/1.4869277>]

Magnetic nanoparticles (NPs) have attracted an increased interest for their applications in nanotechnologies<sup>1</sup> and in the medical field, in particular, for drug targeting, bio-separation, hyperthermia, and MRI imaging.<sup>2–4</sup> Magnetite (Fe<sub>3</sub>O<sub>4</sub>) NPs are excellent candidates for these medical applications, because of their non-toxicity, and their ability to be highly functionalized.<sup>5</sup> Naturally found in minerals, iron oxides have been widely studied and used for many magnetic applications. Magnetite, Fe<sub>3</sub>O<sub>4</sub>, exhibits a high Curie temperature around 850 K, as well as an interesting metal-insulator transition (Verwey transition) at  $T \sim 120$  K.<sup>6</sup> With the emerging interest for magnetic NPs and given the diversity of the preparation methods, there is knowledge to be gained concerning the electronic and magnetic properties of Fe<sub>3</sub>O<sub>4</sub> NPs. In particular, it is unclear if the magnetic moment carried by Fe<sub>3</sub>O<sub>4</sub> is affected by the nanostructuration. In this paper, we report measurements of the spin and orbital moments of Fe<sub>3</sub>O<sub>4</sub> NPs, ranging from 5 to 11 nm in size, using the technique of X-ray Magnetic Circular Dichroism (XMCD).

As most commonly reported, the crystallographic structure of Fe<sub>3</sub>O<sub>4</sub> is associated to an inverse spinel structure.<sup>7</sup> Each Fe<sub>3</sub>O<sub>4</sub> unit includes three types of Fe ions: a Fe<sup>2+</sup> located at an octahedrally coordinated site (B-site), carrying a spin of  $4\mu_B$ , a Fe<sup>3+</sup>, also located at a B-site, carrying a spin of  $5\mu_B$ , coupled in parallel to the Fe<sup>2+</sup> spin, and a Fe<sup>3+</sup>, located at a tetrahedrally coordinated site (A-site) and carrying a magnetic moment of  $-5\mu_B$ , in the direction antiparallel to the first two spins.<sup>8</sup> This configuration leads to a theoretical total

spin moment of  $4\mu_B$  per formula unit (f.u.). Moreover, the orbital moment of Fe<sub>3</sub>O<sub>4</sub> has been found to be quenched.<sup>9,10</sup>

We used different variations of an organic solution method to fabricate the magnetite NPs. See supplementary material<sup>22</sup> for a description of the sample fabrication. Transmission electron microscopy (TEM) and X-ray diffraction (XRD) measurements were carried out to study the structure and size distribution of the NPs. See supplementary material<sup>22</sup> for a detailed account of the results including TEM images and XRD patterns. We report XMCD results for three different NP sizes: sample A, with an average size of 11 nm, sample B, with an average size of 8 nm, and sample C, with an average size of 5.5 nm.

We measured the bulk magnetic behavior of our Fe<sub>3</sub>O<sub>4</sub> NPs by vibrating sample magnetometry (VSM). Fig. 1 displays the magnetization curves for samples A, B, and C, measured at 300 K and at 80 K. The magnetization curves at 300 K indicate a superparamagnetic behavior, with practically no hysteresis, suggesting the absence of significant magnetic coupling between the particles. It is observed that the three samples have different susceptibilities. Given the smoothness of the curves, a sharp estimation of a saturation field is unpractical. Instead, we provide an estimate for the field  $H_{0.9}$  at which 90% of the magnetization at saturation  $M_s$  is reached at 300 K:  $H_{0.9} = 4.2$  kOe, 6.2 kOe, and 12.3 kOe, for samples A, B, and C, respectively. Sample C exhibits the highest  $M_s \sim 70$  emu/g at 80 K. The  $M_s$  values for samples A and B are much lower, on the order of 20 emu/g, but are most likely underestimated because of an overestimation of the mass the samples due to their wetness.

To measure the spin and orbital magnetic moments, we used the XMCD technique.<sup>11–14</sup> Unlike magnetometry,

<sup>a)</sup>Electronic mail: kchesnel@byu.edu

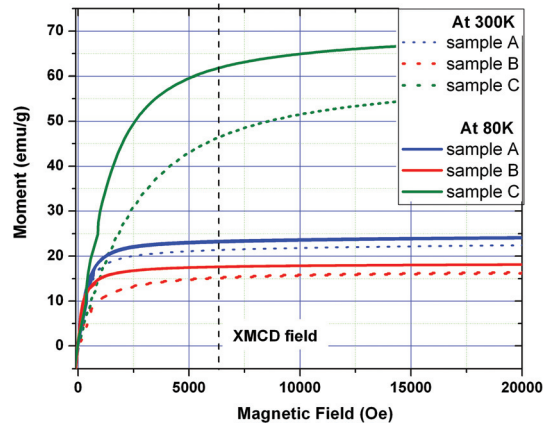


FIG. 1. Magnetization curves measured by VSM for the three samples at 300 K and 80 K.

XMCD is element specific. Orbital and spin contributions to the magnetic moment can be separated by using sum rules.<sup>15</sup> We carried out our x-ray absorption spectroscopy (XAS) measurements at beamline 13-3 of the Stanford Synchrotron Radiation Lightsource (SSRL), at the Stanford Linear Accelerator Center (SLAC). We used circularly polarized soft X-ray light, produced by an elliptical polarization undulator, with a degree of polarization of 98%. The light was finely tuned to the  $L_{2,3}$  absorption edges of Fe, using a 11001/mm spherical grating monochromator with an energy resolution of 0.2 eV around 700 eV. For this measurement, the  $\text{Fe}_3\text{O}_4$  NPs were deposited on 50 nm thick  $\text{Si}_3\text{N}_4$  membranes, with a window size of  $100 \times 100 \mu\text{m}$ . The membranes were mounted in transmission geometry onto a cryogenic sample holder in a vacuum chamber. The size of the beam at the location of the sample was about  $220 \mu\text{m} \times 70 \mu\text{m}$ , thus illuminating most of the window and providing a fairly good statistics. A magnetic field was applied *in-situ*, in the direction parallel to the beam and perpendicular to the membranes, up to 6.3 kOe. X-ray absorption spectroscopy (XAS) were first recorded by scanning the energy across the Fe  $L_{2,3}$  edges, from 690 eV to 735 eV.

XAS absorption spectra were carefully normalized in a way to remove the background slopes below the  $L_3$  edge and above the  $L_2$  edge that are due to charge absorption, and the  $L_{3,2}$  absorption edge jump was normalized to 1. The XMCD signal was obtained by subtracting the normalized XAS signals measured at opposite helicities. Fig. 2(a) shows the XAS absorption spectra for sample B at 300 K, along with the extracted XMCD signal. Fig. 2(b) shows the measured XMCD signal for the three samples, at 300 K and 80 K.

The spin and orbital magnetic moments were calculated, per  $\text{Fe}_3\text{O}_4$  unit, using the following sum rules:<sup>15,16</sup> See supplementary material for a description of the sum rules in our calculation.<sup>22</sup> Table I displays the values of the orbital and spin moments,  $M_L$  and  $M_S$ , for our three samples, at 300 K and 80 K. The moments are here calculated for the whole unit  $\text{Fe}_3\text{O}_4$ . The net magnetic moment of iron per  $\text{Fe}_3\text{O}_4$  unit has been estimated by adding the orbital and spin components  $M_{Fe} = M_L + M_S$ . Also, the XMCD signal was measured at a field of 6.3 kOe, which is slightly below saturation point for all samples, therefore the NPs were not fully saturated. We therefore extrapolated  $M_{Fe}$  to its value at saturation, using the ratio found in the magnetization curve between the magnetization  $M_{6.3\text{kG}}$  at 6.3 kOe and the magnetization at saturation  $M_{sat}$  (estimated at 50 kOe). Given the noisiness of the XAS and XMCD data, we believe the error on our estimation of  $M_S$  is around  $\pm 0.1 \mu_B$ .

Our measured values for the orbital and spin components, reported in Table I, suggest a quenching of the orbital moment ( $M_L \sim 0$ ) for all the three samples, both at 300 K and at 80 K. This orbital quenching agrees with theoretical calculations<sup>17,18</sup> and experimental observations in  $\text{Fe}_3\text{O}_4$  single crystal<sup>8</sup> as well as in other  $\text{Fe}_3\text{O}_4$  nanoparticles.<sup>19,20</sup> It appears that the quenching of the orbital moment remains unaffected by the nanostructuration. The values for the spin component  $M_S$  and the resulting net magnetic moment  $M_{Fe}$  are significantly higher than  $M_L$ , but somewhat lower than the  $M_{Fe}$  values reported elsewhere for bulk  $\text{Fe}_3\text{O}_4$ <sup>8,17,18</sup> and other  $\text{Fe}_3\text{O}_4$  NPs.<sup>19</sup> Various reasons could explain the lowering effect. First, these values may be underestimated because

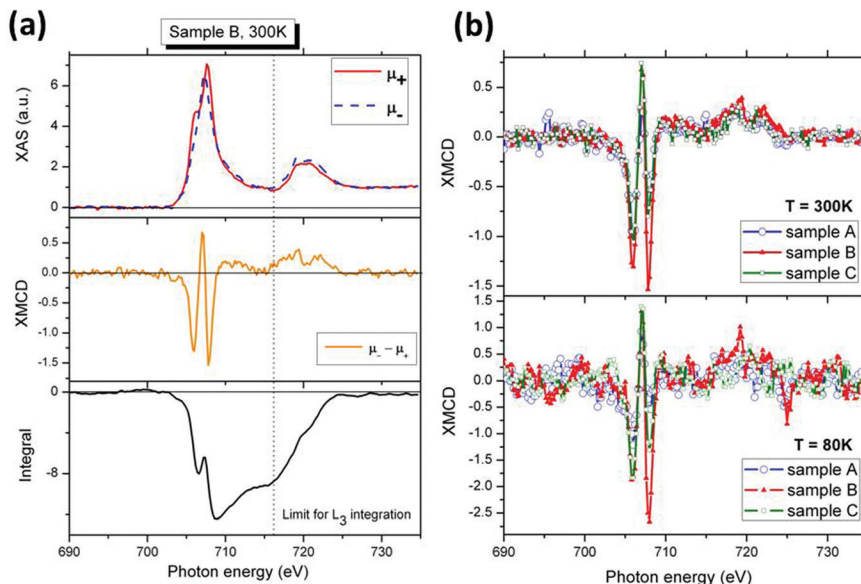


FIG. 2. (a) XAS spectra for sample B at 300 K measured at opposite helicities, and the resulting XMCD signal, along with its integral; (b) Comparison of the XMCD signal for the three samples A, B, and C at 300 K and 80 K.

TABLE I. Calculated values for the orbital and spin contributions to the magnetic moment  $M_{Fe}$ .

Sample	Particle size (nm)	Values measured at H = 6300 Oe (per Fe <sub>3</sub> O <sub>4</sub> formula unit) <sup>a</sup>						Extrapolated values at saturation <sup>b</sup>	
		Orbital $M_L$ ( $\mu_B$ )		Spin $M_S$ ( $\mu_B$ )		Total $M_{Fe}$ ( $\mu_B$ )		Total $M_{Fe}$ ( $\mu_B$ )	
		300 K	80 K	300 K	80 K	300 K	80 K	300 K	80 K
Sample A	11.3 ± 2.5	0.07(5)	0.06(6)	2.09	2.36	2.16	2.43	2.33	2.57
Sample B	8.1 ± 1.7	0.01(5)	0.02(7)	2.26	2.59	2.27	2.62	2.47	2.72
Sample C	5.6 ± 1.0	0.03(8)	0.03(7)	1.45	1.70	1.49	1.74	1.91	1.98

<sup>a</sup>These values are calculated based on a number of hole  $N_h = 13.7$ .

<sup>b</sup>The values for the total magnetic moment  $M_{Fe}$  are extrapolated using the ratio  $M_{sat}/M_{0.63T}$  given by the VSM magnetization curves. At 300 K, the ratios are 1.08, 1.09, and 1.28 for samples A, B, and C, respectively; at 80 K, the ratios are 1.06, 1.04, and 1.14, respectively.

of the limited range of photon energy used to integrate our XMCD spectra—it has been shown that extending the range of energy for the signal integration above the  $L_2$  edge increases the estimation of  $M_S$ .<sup>8</sup> Second, the value which we have used for the number of holes  $N_h = 13.7$  is based on local spin-density approximation (LDA) calculation for bulk Fe<sub>3</sub>O<sub>4</sub>, may be underestimated in the case of NPs, as the presence of a ligand shell surrounding each particle may modify the electronic structure at the surface. Third, the lowering of the  $M_{Fe}$  in NPs compared to bulk Fe<sub>3</sub>O<sub>4</sub> may be in part real: it could be due to nanostructural effects, further oxidation at the surface of the particles, and the presence (undetectable by XRD) of maghemite  $\gamma$ -Fe<sub>2</sub>O<sub>3</sub>, which would contribute to lower the average value of  $M_{Fe}$ .<sup>21</sup>

The measured values of magnetic moment  $M_{Fe}$  vary significantly between our samples and when changing temperature.  $M_{Fe}$  increases when cooling from 300 K down to 80 K, by about 10% for samples A and B, and 3% for sample C. This increase somewhat contradicts experimental XMCD results in bulk Fe<sub>3</sub>O<sub>4</sub> that indicate no significant change of  $M_S$  nor  $M_L$  with temperature.<sup>8</sup> In our case, the increase of  $M_S$  and  $M_{Fe}$  at low temperature seems real as it is observed in all the three samples, and it mimics the increase of the magnetization observed in the VSM magnetization curves. We suggest that this increase of  $M_{Fe}$  with cooling is essentially due to thermal fluctuations in the NP assemblies, which arises from their superparamagnetic nature. Moreover, the measured value for  $M_{Fe}$  is found to be about 28% lower in sample C, than in sample B. This difference may be due to the change in particle size. Our results suggest that  $M_{Fe}$  significantly decrease when particles become small, in the order of a few nanometers, and surface spin-disorder effects may become more predominant.

In conclusion, we have measured orbital and spin contributions to the magnetic moment in three types of organically prepared Fe<sub>3</sub>O<sub>4</sub> nanoparticles ranging from 5 to 11 nm in size. To our knowledge, only a few XMCD studies have been performed on Fe<sub>3</sub>O<sub>4</sub> NPs.<sup>19,20</sup> Given the diversity of the NP shapes, sizes, and environments, results can vary significantly and there is still much to learn. Our results indicate that while the magnetic moment  $M_{Fe}$  in the larger nanoparticles appears somewhat close to  $M_{Fe}$  in Fe<sub>3</sub>O<sub>4</sub> single crystal, it may be reduced by a number of factors associated with the

nanostructuring: the preparation method to fabricate the nanoparticles, which may lead to various degrees of purity of Fe<sub>3</sub>O<sub>4</sub>, with presence of maghemite, the particle environment, with a ligand shell that may alter the electronic properties at the surface, but also the particle shape and size, potentially leading to an increased fractional volume of an oxidized shell when the particles are reduced to a few nanometers in size.

We thank Stacey Smith and Branton Campbell for useful discussion, and Jeffrey Farrer for help with TEM imaging. This research was supported by the ORCA office at BYU, as well as by the DOE Office of Basic Energy Sciences, Materials Sciences and Engineering Division, under Contract No. DE-AC02-76SF00515. Portions of this research were carried out at the Stanford Synchrotron Radiation Lightsource, a Directorate of SLAC National Accelerator Laboratory and an Office of Science User Facility operated for the U.S. Department of Energy Office of Science by Stanford University.

- <sup>1</sup>N. A. Frey *et al.*, *Chem. Soc. Rev.* **38**, 2532 (2009).
- <sup>2</sup>S. Mornet *et al.*, *J. Mater. Chem.* **14**, 2161 (2004).
- <sup>3</sup>E. Duguet *et al.*, *Nanomedicine* **1**(2), 157 (2006).
- <sup>4</sup>J. H. Gao *et al.*, *Acc. Chem. Res.* **42**(8), 1097 (2009).
- <sup>5</sup>A. Ito *et al.*, *J. Biosci. Bioeng.* **100**, 1 (2005).
- <sup>6</sup>E. J. Verwey, *Nature (London)* **144**, 327 (1939).
- <sup>7</sup>M. E. Fleet, *Acta Crystallogr., Sect. B: Struct. Crystallogr. Cryst. Chem.* **37**, 917–920 (1981).
- <sup>8</sup>E. Goering *et al.*, *Europhys. Lett.* **73**(1), 97–103 (2006).
- <sup>9</sup>E. Goering *et al.*, *Phys. Rev. Lett.* **96**, 039701 (2006).
- <sup>10</sup>H.-T. Jeng and G. Y. Guo, *Phys. Rev. B* **65**, 094429 (2002).
- <sup>11</sup>G. Schütz *et al.*, *Phys. Rev. Lett.* **58**, 737 (1987).
- <sup>12</sup>B. T. Thole *et al.*, *Phys. Rev. Lett.* **68**(12), 1943 (1992).
- <sup>13</sup>P. Carra *et al.*, *Phys. Rev. Lett.* **70**, 694 (1993).
- <sup>14</sup>J. Stöhr, *J. Magn. Magn. Mater.* **200**, 470–497 (1999).
- <sup>15</sup>C. T. Chen *et al.*, *Phys. Rev. Lett.* **75**, 152 (1995).
- <sup>16</sup>C. Piamonteze *et al.*, *Phys. Rev. B* **80**, 184410 (2009).
- <sup>17</sup>D. J. Huang *et al.*, *Phys. Rev. Lett.* **93**, 7 (2004).
- <sup>18</sup>E. J. Goering *et al.*, *J. Magn. Magn. Mater.* **310**, e249 (2007).
- <sup>19</sup>N. Pérez *et al.*, *Appl. Phys. Lett.* **75**, 152 (2004).
- <sup>20</sup>A. Yamasaki *et al.*, *J. Phys.: Conf. Ser.* **150**, 042235 (2009).
- <sup>21</sup>D. Ortega *et al.*, *Philos. Trans. R. Soc., A* **368**, 4407 (2010).
- <sup>22</sup>See supplementary material at <http://dx.doi.org/10.1063/1.4869277> for a description of the sample fabrication; a detailed account of the results including TEM images and XRD patterns; and a description of the sum rules in our calculation.